第 30 卷 第 10 期　焊 接 学 报　Vol. 30 No. 10
2009 年 10 月　TRANSACTIONS OF THE CHINA WELDING INSTITUTION　October 2009

不锈钢电弧辅助活性 TIG 焊

黄　勇，　樊　　,丁　林　涛，　雒焕胜
（兰州理工大学 甘肃省有色金属新材料国家重点实验室，兰州　730050）

摘　要：针对不锈钢，提出了一种新型活性 TIG 焊方法——电弧辅助活性 TIG 焊，即 AA-TIG 焊（arc assisted activating TIG welding）．该焊接方法通过在正常 TIG 焊前以活性混合气体作为保护气体，采用小电流钨极电弧预熔待焊焊道表面，可使熔深显著增加，焊接效率大大提高，而且具有可全自动化焊接和工艺可重复性好等优点．分别采用 O_2＋Ar，CO_2＋Ar，空气作为小电流钨极电弧的保护气体进行了单弧 AA-TIG 焊．与传统 TIG 焊比较，发现 O_2＋Ar，CO_2＋Ar 和空气都可显著增加熔深，减小熔宽，焊缝表面成形良好．采用 CO_2＋Ar 作为活性混合保护气体进行双弧 AA-TIG 焊，焊缝成形良好，熔深显著增加．熔深随着焊枪间距减小而增大．

关键词：不锈钢；活性 TIG 焊；AA-TIG 焊；活性混合气体；自动化焊接
中图分类号：TG444　文献标识码：A　文章编号：0253－360X（2009）10－0001－04

黄　勇

0　序　言

TIG 焊是现代生产制造中广泛应用的一种惰性气体保护焊，是常规焊接方法中高质量焊接的代表．但由于受到钨极载流能力的限制以及电弧热不集中的影响，该方法存在着焊接熔深浅、生产效率低等缺点，从而限制了它的应用领域．自 20 世纪 90 年代以来，A-TIG 焊作为活性化焊接技术的代表，引起了人们广泛关注[1－5]．它通过在传统 TIG 焊前将很薄的一层表面活性剂（简称 A-TIG 焊活性剂）涂敷在施焊板材表面可使得焊接熔深显著增加．但在实际应用中，由于生产过程中增加一道活性剂涂敷工序，使得生产效率大大降低，并且通常采用手工刷涂的办法进行活性剂涂敷，不易保证涂敷质量，影响了工艺稳定性．所以自其产生以来还未在实际生产中得到广泛应用．

通过改变活性元素的引入方式，提出了一种新型活性 TIG 焊方法——电弧辅助活性 TIG 焊，即 AA-TIG 焊（arc assisted activating TIG welding）．该焊接方法通过在正常 TIG 焊前以活性混合气体作为保护气体，采用小电流钨极电弧预熔待焊焊道表面，可使熔深显著增加，生产效率大大提高，而且具有可全自动化焊接和工艺可重复性好等优点．根据实际情况，AA-TIG 焊既可采用单弧焊接工艺，也可采用双弧焊接工艺，即小电流钨极电弧预熔处理和常规 TIG 焊同时进行，从而可进一步增加熔深，减少工序，提高生产效率．

分别采用 O_2＋Ar，CO_2＋Ar 和空气作为小电流钨极电弧的保护气体进行单弧 AA-TIG 焊，并以 CO_2＋Ar 作为小电流钨极电弧的保护气体，通过改变焊枪之间的间距，进行双弧 AA-TIG 焊，分析了焊缝成形和焊缝组织的变化规律，研究了 AA-TIG 焊的工艺可行性．这对于加深对活性焊接法的认识，推广应用 AA-TIG 焊具有重要意义．

1　试验方法

选用不锈钢 304 作为试板母材，板厚为 10 mm．单弧 AA-TIG 焊时，小电流钨极电弧预熔处理采用的活性混合气体分别为 O_2＋Ar，CO_2＋Ar 和空气，其中 O_2，CO_2 和氩气纯度为 99.9%．采用空气作为保护气体时，直接在空气中引燃电弧进行焊接．双弧 AA-TIG 焊时，活性混合气体为 CO_2＋Ar．

试验前机械加工试件，并用酒精擦拭以除去表面油污．为了保证试验数据的一致性与可比性，必须保证焊接过程中所有焊接工艺参数精确设定和焊枪精确沿着试件中心线行走，并且 TIG 焊和 AA-TIG 焊一次焊接完成．焊后，采用标准金相制备法处理试件，并用数码相机记录焊缝表面和截面形貌，分析活

收稿日期：2008－07－25
基金项目：教育部春辉计划（Z2005－1－62007）；教育部博士学科点专项基金资助项目（20040731001）

性混合气体对焊缝表面成形的影响. 采用大型光学显微镜 MEF3 分析活性混合气体对焊缝组织的影响.

单弧 AA-TIG 焊时,先进行小电流钨极电弧预熔处理,焊缝长度为整体焊道长度的一半,工艺参数如表1 所示. 然后进行正常 TIG 焊,焊接工艺参数如表2 所示. 双弧 AA-TIG 焊时,一前一后布置两把 TIG 焊枪,前一把焊枪进行小电流钨极电弧预熔处理,后一把焊枪进行正常 TIG 焊. 两把 TIG 焊枪之间的间距分别为 25 和 30 mm. 焊接时两把焊枪同时起弧和灭弧. 焊接工艺参数除常规 TIG 焊焊接速度变为 125 mm/min 外,其余焊接工艺参数与单弧焊接时相同.

表1 小电流钨极电弧的焊接工艺参数

Table 1 Experimental parameters of low current tungsten electrode arc

焊接电流 I/A	预熔速度 v/(mm·min^{-1})	弧长 L/mm	氩气流量 q_{v1}/(L·min^{-1})	活性气体流量 q_{v2}/(L·min^{-1})
60	125	4	7.5	2

表2 常规 TIG 焊的焊接工艺参数

Table 2 Welding parameters of conventional TIG welding

焊接电流 I/A	焊接速度 v/(mm·min^{-1})	弧长 L/mm	氩气流量 q_{v1}/(L·min^{-1})
200	100	3	12.5

2 试验结果

2.1 单弧 AA-TIG 焊

2.1.1 焊缝表面成形

从图 1 可以看出,三种混合气体所得焊缝表面成形都良好,其中以 CO_2+Ar 为最好,焊缝有一定余高,表面平滑,波纹细腻,焊渣呈点状分布,少而均匀. 而 O_2+Ar 和空气所得焊缝表面的焊渣呈小片状零星分布.

(a) O_2+Ar

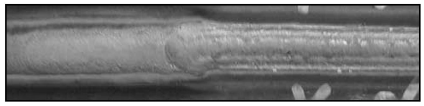

(b) CO_2+Ar

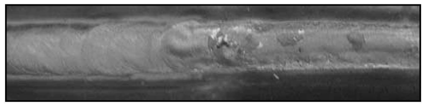

(c) 空气

图1 混合气体种类对焊缝表面成形的影响

Fig 1 Effect of mixing shielding gases on weld surface appearance

2.1.2 焊缝熔深熔宽

从图 2 可以看出,三种混合气体都能明显增加熔深,减小熔宽,而且焊缝熔深熔宽分别都很相近,熔深大约为传统 TIG 焊的 1.9 倍左右,而熔宽大约为 0.8 倍左右.

2.1.3 焊缝组织

从图 3 可以看出,三种活性混合气体对焊缝区显微组织的影响并不相同. 与传统 TIG 焊相比较,O_2+Ar 使得焊缝区显微组织有所粗化,CO_2+Ar 对焊缝区显微组织几乎没有影响,空气使得焊缝区显微组织明显细化.

2.2 双弧 AA-TIG 焊

2.2.1 电弧形貌

从图 4 可以看出,进行双弧 AA-TIG 焊时,小电流钨极电弧由于电弧电流小,弧长长,电弧挺度差,焊接时电弧偏向正常 TIG 电弧方向. 随着焊枪间距增加,电弧挺度变差,电弧中心等离子区变宽;而焊枪间距变化对正常 TIG 焊电弧几乎没有影响.

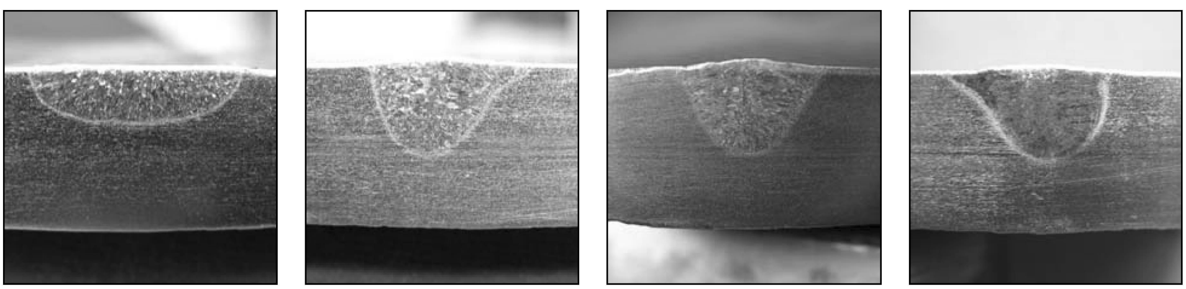

(a) TIG焊　(b) O_2+Ar　(c) CO_2+Ar　(d) 空气

图2 混合气体种类对焊缝熔深熔宽的影响

Fig 2 Effect of mixing shielding gases on weld penetration and weld width

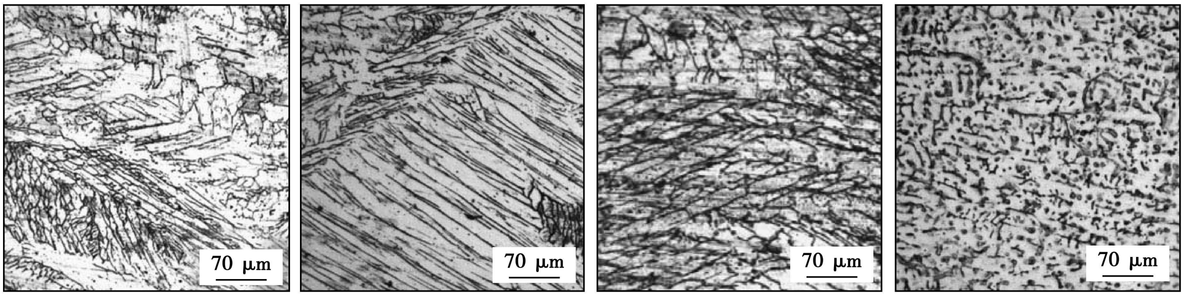

(a) TIG焊　(b) O_2+Ar　(c) CO_2+Ar　(d) 空气

图 3　混合气体种类对焊缝显微组织的影响

Fig. 3　Effect of mixing shielding gases on weld onicrostructure

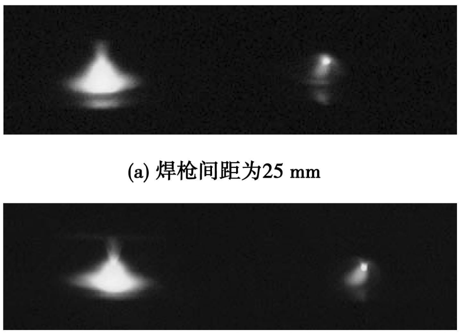

(a) 焊枪间距为25 mm

(b) 焊枪间距为30 mm

图 4　双弧 AA-TIG 焊时的电弧形貌

Fig. 4　Arc appearances of dual-arc AA-TIG welding

2.2.2　焊缝表面成形

图5为双弧 AA-TIG 焊时的焊缝表面形貌．沿着从左往右的焊接方向，整条焊缝分为三个区域：最左侧为正常 TIG 焊焊缝区，最右侧为小电流钨极电弧预熔处理区，中间区域为AA-TIG 焊焊缝区．可以看出，在两种焊枪间距情况下，AA-TIG 焊的焊缝表面成形都良好，表面平滑，波纹细腻，焊渣呈小片状均匀分布在焊缝表面．与传统 TIG 焊相比，AA-TIG 焊的焊缝宽度没有明显变化，但余高明显增加．在正常TIG焊区域和AA-TIG焊区域的交界处存在一个扇形区，区域两端余高较高，而中间部位余高较小．在扇形区域内，几乎没有焊渣分布．

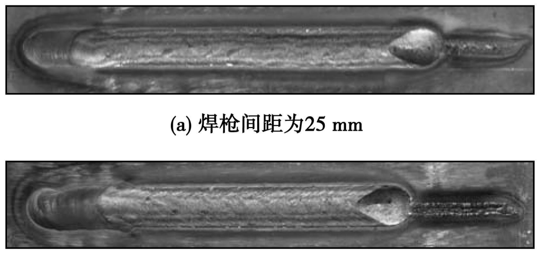

(a) 焊枪间距为25 mm

(b) 焊枪间距为30 mm

图 5　双弧 AA-TIG 焊时的焊缝表面形貌

Fig 5　Weld surface appearances of dual-arc AA-TIG welding

2.2.3　焊缝熔深熔宽

从图6可以看出，采用双弧工艺时，焊缝熔深显著增加．焊枪间距为 30 mm 时，双弧 AA-TIG 焊的熔深为常规 TIG 焊的 2.0 倍，而当焊枪间距为 25 mm 时，大约为 2.3 倍，即随着焊枪间距减小，熔深增加．

2.2.4　焊缝组织

从图7可以看出，采用双弧焊接工艺，由于小电流钨极电弧的预热作用，在两种焊枪间距情况下，焊缝区显微组织都略有粗化．

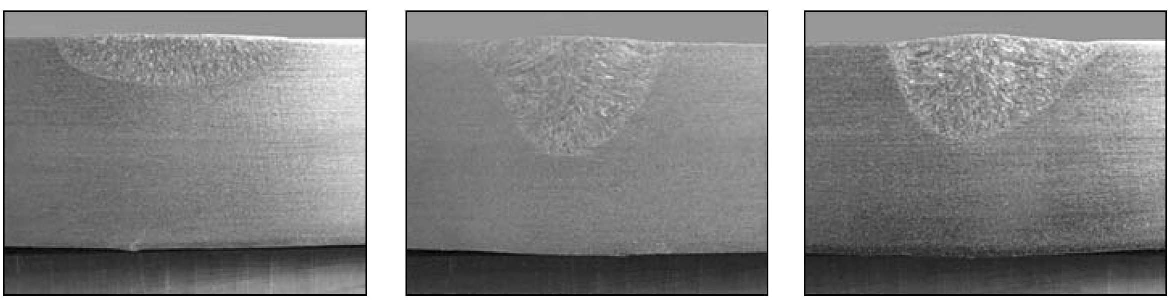

(a) TIG焊　(b) AA-TIG焊(25 mm)　(c) AA-TIG焊(30 mm)

图 6　焊枪间距对双弧焊熔深熔宽的影响

Fig. 6　Effect of welding torch distance on weld penetration and weld width

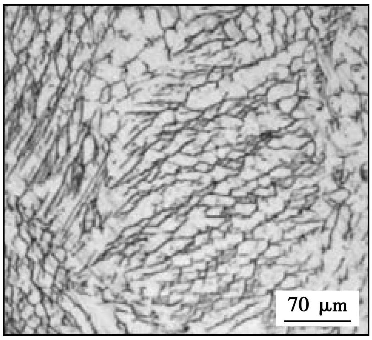

(a) TIG焊

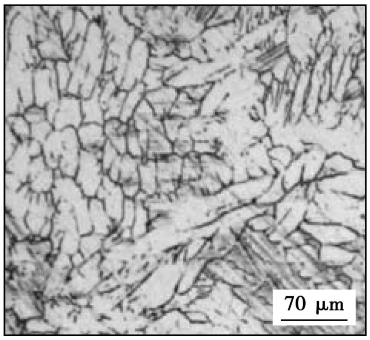

(b) AA–TIG焊(25 mm)

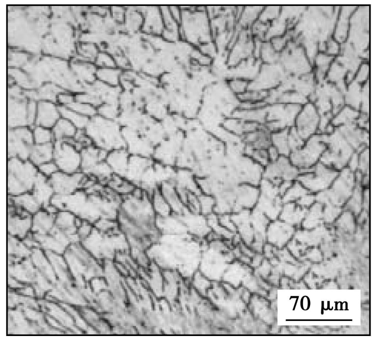

(c) AA–TIG焊(30 mm)

图 7 双弧焊时的焊缝区显微组织

Fig 7 Weld zone microstruoture of dual-arc AA-TIG welding

3 分析与讨论

关于不锈钢活性 TIG 焊时熔深增加的机理, 现在越来越多的人[3-7]认为是由于表面活性元素的引入使得熔池表面张力温度梯度改变, 从而导致熔池内液态金属流态改变, 最终熔深增加.

以往活性焊接中活性元素的引入方式主要有两种, 一是在工件表面涂敷活性剂, 即进行 A-TIG 焊; 二是在惰性保护气体中添加入 O_2 或者 CO_2 等活性气体, 即进行活性混合气体保护焊[6]. 进行 A-TIG 焊时, 由于一般采用手工刷涂的办法进行活性剂涂覆, 除了活性剂成本高外, 涂敷效率也较低, 涂敷质量不易保证. 而采用活性混合气体保护焊虽然提高了焊接效率, 降低了焊接成本, 但由于只有当混合气体中 O_2 或者 CO_2 气体体积百分数在 0.3%~0.5% 时才能起到增加熔深的作用[6,7], 混合气体中活性气体含量非常少, 这就要求气体混合装置具有很高精度, 使得设备成本高. 而且由于有效作用区间小, 焊接过程容易受到外界干扰, 工艺稳定性差.

AA-TIG 焊改变了活性元素引入方式, 采用活性混合气体进行小电流钨极电弧预熔待焊焊道表面, 在待焊焊道表面形成氧化层, 从而彻底克服了以上两种传统方式的缺点, 实现了自动化焊接生产, 提高了焊接效率, 保证了工艺可重复性. 尤其当改进焊枪结构实现双弧焊接工艺后, 将进一步简化焊接工序, 增加焊接熔深, 提高生产效率. 从试验结果来看, 熔深对小电流钨极电弧预熔处理时的活性混合气体种类不敏感, 从而使得该工艺具有很好的适应性.

4 结 论

(1) 提出了一种新型不锈钢活性焊接法——电弧辅助活性 TIG 焊, 即 AA-TIG 焊 (arc assisted activating TIG welding). 它通过在正常 TIG 焊前以活性混合气体作为保护气体, 采用小电流钨极电弧预熔待焊焊道表面, 可使熔深显著增加, 生产效率大大提高, 而且具有可全自动化焊和工艺可重复性好等优点.

(2) 采用 O_2+Ar, CO_2+Ar 和空气作为活性混合保护气体进行单弧 AA-TIG 焊, 都可明显增加熔深和减小熔宽, 焊缝成形良好. 而且对于这三种混合气体, 焊缝熔深熔宽都很相近.

(3) 采用 CO_2+Ar 作为活性混合保护气体进行双弧 AA-TIG 焊, 焊缝成形良好, 熔深显著增加. 熔深随着焊枪间距减小而增大.

参考文献:

[1] Tanaka M, Shimizu T, Terasaki H, *et al*. Effects of activating flux on arc phenomena in gas tungsten arc welding[J]. Science and Technology of Welding and Joining, 2000, 5(6): 397-402.

[2] 刘凤尧. 不锈钢和钛合金活性剂焊接和熔深增加机理的研究[D]. 哈尔滨: 哈尔滨工业大学博士学位论文, 2003.

[3] Heiple C R, Roper J R. Mechanism for minor element effect on TIG fusion zone geometry[J]. Welding Journal, 1982, 61(4): 97-102.

[4] Dong C, Katayama S. Basic understanding of A-TIG welding process[C]// Masao Toyota. Technical Trends and Future Prospectives of Welding Technology for Transportation, Land, Sea, Air and Space. Osaka, Japan: IIW, 2004: 371-382.

[5] 张瑞华. 活性焊接法及熔深增加机理的数值模拟研究[D]. 兰州: 兰州理工大学博士学位论文, 2005.

[6] Lu Shanping, Fujii H, Nogi K. Marangoni convection and weld shape variations in Ar-O_2 and Ar-CO_2 shielded GTA welding[J]. Materials Science and Engineering A, 2004, 380: 290-297.

[7] Lu Shanping, Fujii H, Nogi K. Sensitivity of marangoni convection and weld shape variations to welding parameters in O_2-Ar shielded GTA welding[J]. Scripta Materialia, 2004, 51(3): 271-277.

作者简介: 黄 勇, 男, 1972 年出生, 副教授, 博士. 主要从事活性焊接技术研究. 发表论文 25 篇.

Email: hyorhot@lut.cn

MAIN TOPICS, ABSTRACTS & KEY WORDS

Arc assisted activating TIG welding process for stainless steels

HUANG Yong, FAN Ding, LIN Tao, LUO Huansheng (State Key Laboratory of Gansu Advanced New Non-ferrous Metal Materials, Lanzhou University of Technology, Lanzhou 730050, China). p 1—4

Abstract: A new activating TIG welding process for stainless steels called AA-TIG (arc assisted activating TIG) welding is proposed. The weld surface is pre-melted by low current tungsten arc with activating mixing shielding gas before normal TIG welding, which can dramatically improve weld penetration and production efficiency and ensure the repeatability of welding process and automatic welding. O_2 + Ar, CO_2 + Ar and air are respectively used as the shielding gas of pre-melting with low current tungsten electrode arc for single-arc AA-TIG welding; compared with conventional TIG welding, all of the three mixing gases can increase weld penetration and decrease weld width; all of the weld appearances are fine. When CO_2 + Ar mixing gas is used as the shielding gas of low current tungsten electrode arc in dual-arc AA-TIG welding, the weld forming is fine, the weld penetration is improved dramatically, but the weld penetration increases as the distance between the welding torches decreases.

Key words: stainless steel; activating TIG welding; AA-TIG welding; activating mixing gas; automatic welding

Effects of electrode wear on weld quality of hot galvanization steel with high strength in resistance spot welding

ZHANG Xuqiang[1], ZHANG Yansong[2], LIU Yancong[1] (1. School of Mechanical Engineering, Petroleum University of China, Dongying 257061, China; 2. School of Mechanical Engineering and Power, Shanghai Jiaotong University, Shanghai 200030, China). p 5—8

Abstract: Electrode wear characteristics were studied; the electrode life of un-coated steels was much lower and pitting changed more obviously than that of galvanization steels when welding. The effect of electrode wear on weld quality was studied; the expulsion was serious and more micro-cracks were grown at early electrode wear stage, which decreased weld quality greatly. And then based on the experiment results of effect of electrode wear on weld quality, welding technique step-current was established according to the current density that micro-crack degree was less than 0.25 mm to reduce the effect of electrode wear on weld quality.

Key words: electrode wear; hot galvanization steel with high strength; weld quality; resistance spot welding

Temperature distribution of Al/Ti dissimilar alloys joint in laser welding brazing

FENG Xiaosong[1], CHEN Shuhai[2], LI Liqun[2], CHEN Yanbin[2] (1. College of Material Science and Technology, Nanjing University of Aeronautics and Astronautics, Nanjing 210016, China; 2. State Key Laboratory of Advance Welding Production Technology, Harbin Institute of Technology, Harbin 150001, China). p 9—12, 16

Abstract: Laser welding-brazing experiments of 5A06 and TC4 were carried out and AlSi12 was used as filler metal. The heat transfer in the process was analyzed and the three heat source models were established. With the heating of laser vertical beam, declining beam, off-center beam and rectangular beam, the joint temperature field of Al/Ti dissimilar alloys was calculated and analyzed by finite element method. The simulated results indicate that the temperature distribution is dissymmetrical obviously on the two sides of the seam. It can avoid the local overheating at the interface of titanium alloy that the laser spot center deviation from the seam centerline to aluminum base metal side is 0.4—0.6 mm. With elliptical spot heating, the temperature history of the joint is similar with the situation of circle spot heating, and with rectangular spot heating, the temperature difference between the joint ! interface upper part and bottom is reduced.

Key words: laser welding-brazing; dissimilar alloys; temperature field; numerical simulation

Microstructure of a novel Al-based amorphous reinforced aluminum metal matrix composite

LIU Peng[1,2], SHI Qingyu[2], BIAN Xiufang[3], XU Shubo[1], REN Guocheng[1] (1. School of Materials Science and Engineering, Shandong Jianzhu University, Jinan 250101, China; 2. Department of Mechanical Engineering, Tsinghua University, Beijing 100084, China; 3. Key Laboratory of Liquid Structure and Heredity of Materials, Ministry of Education, Shandong University, Jinan 250061, China). p 13—16

Abstract: A novel aluminium metal matrix composite reinforced with Al-based amorphous was fabricated by friction stir processing. The microstructure, microhardness and chemical composition of the composite were analyzed by metallography, microsclemeter and scanning electron microscope. The test results indicate that the composite is composed of an obvious sandwich structure including amorphous strip and base material. The hardness of the composite is higher than that of base metal. The phase constituents of the composite are composed of α-Al, Mg_2Al_3, $MnAl_6$ and La_3Al_{11}. An obvious crystallization characteristic occurs in the original amorphous strip of the composite, in which the crystallization process may be effected by thermal friction, mechanical stirring and pressure forces.

Key words: metal matrix composites; friction stir processing; amorphous alloy; microstructure; hardness